

Dynamical Fermion Masses and Constraints of Gauge Invariance in Quenched QED3

A. Bashir[†], A. Raya[‡]

[†]*Instituto de Física y Matemáticas, Universidad Michoacana de San Nicolás de Hidalgo, Apartado Postal 2-82, Morelia, Michoacán 58040, México.*

[‡]*Facultad de Ciencias, Universidad de Colima, Bernal Díaz del Castillo #340, Col. Villa San Sebastián, Colima, Colima 28045, México.*

Numerical study of the Schwinger-Dyson equation (SDE) for the fermion propagator (FP) to obtain dynamically generated chirally asymmetric solution in an arbitrary covariant gauge ξ is a complicated exercise specially if one employs a sophisticated form of the fermion-boson interaction complying with the key features of a gauge field theory. However, constraints of gauge invariance can help construct such a solution without having the need to solve the Schwinger-Dyson equation for every value of ξ . In this article, we propose and implement a method to carry out this task in quenched quantum electrodynamics in a plane (QED3). We start from an approximate analytical form of the solution of the SDE for the FP in the Landau gauge. We consider the cases in which the interaction vertex (i) is bare and (ii) is full. We then apply the Landau-Khalatnikov-Fradkin transformations (LKFT) on the dynamically generated solution and find analytical results for arbitrary value of ξ . We also compare our results with exact numerical solutions available for a small number of values of ξ obtained through a direct analysis of the corresponding SDE.

PACS numbers: 11.15.Tk, 12.20.-m

I. INTRODUCTION

Quantum electrodynamics in a plane (QED3) continues to attract attention both in the field of superconductivity, e.g., [1], where it has been used in the study of high T_c superconductors, as well as in the realm of dynamical generation of fundamental fermion masses where the numerical findings on the lattice and the results obtained by employing Schwinger-Dyson equations (SDE), [2], are yet to arrive at a final consensus.

In this paper, we take up the latter question in the light of SDE. Owing to its simplicity as compared with its four-dimensional counterpart and quantum chromodynamics (QCD), the quenched version of QED3 is particularly neat to unfold the intricacies of the SDE for the fermion propagator (FP). It provides us with an excellent laboratory to study one of its unwelcome features, namely, the lack of gauge invariance of the associated physical observables. It hampers a fully reliable predictive power of the said equations in the non-perturbative regime of interactions. This problem can be traced back to not employing, or doing so incorrectly, the gauge identities such as Ward-Green-Takahashi identities (WGTI) [3], the Nielsen identities (NI) [4] and the Landau-Khalatnikov-Fradkin transformations (LKFT) [5]. In this article, we address this issue in the light of the LKFT.

The LKFT of the Green's functions describe the specific manner in which these functions transform under a variation of gauge. These transformations are non-perturbative in nature, and they are better described in coordinate space. It is primarily for this reason that some earlier works on its implementation in the study of the FP were carried out in the coordinate space, [7]. In the context of gauge technique, the FP in QED4 was found to have correct infrared and ultraviolet behaviour on employing an ansatz for the longitudinal vertex. Momentum

space calculations are more tedious, owing to the complications induced by Fourier transforms. These difficulties are reflected in [8] where non-perturbative FP is obtained starting from a perturbative one in the Landau gauge in QED3 and QED4.

In perturbative calculations of the Green's functions, these transformations are satisfied at every level of approximation. However, in the non-perturbative study of gauge field theories through SDE in an arbitrary covariant gauge, one can ensure these transformations for the FP and the vertex are satisfied only with a correct ansatz for the so-called transverse part of the three point fermion-boson vertex. In practice it implies constructing a very complicated vertex if one wants to obtain correct gauge covariance in all momentum regimes. In QED3, recently an ansatz has been proposed, [6] which guarantees that the resulting FP satisfies its LKFT to two orders and the vertex itself to the first order in their respective perturbative expansions. As LKFT are non-perturbative in nature, we expect them not only to be satisfied at every order in perturbation theory but also in phenomena which are realized only non-perturbatively, such as dynamical chiral symmetry breaking (DCSB).

The continuum studies of DCSB are carried out through the SDE for the FP. Gauge dependence of the FP can be obtained by solving these equations in different covariant gauges. In practice, one needs to go in small steps of the gauge parameter away from the Landau gauge and it is prohibitively difficult to be able to compute the result for an arbitrarily large value of the gauge parameter especially if a sophisticated form of the three point interaction is taken into account, [9, 10]. The LKFT provide us with a mechanism to achieve this goal [11]. What we have to do is to start from the result in the Landau gauge and simply perform an LKFT to find the result in any other gauge.

The paper is organised as follows : In Sect. II we recall the solution of the FP in the Landau gauge employing the bare vertex. In order to get better physical insight, we approximate the solution with a simple analytic parametric form; in Sect. III, we perform the LKFT of the dynamically generated to get the FP in an arbitrary covariant gauge. In Sect. IV we discuss in details various limiting cases of our results. In Sect. V, we go further to implement the full vertex. We present the numerical results in Sect. VI and conclusions in Sect. VII.

II. THE FERMION PROPAGATOR FOR THE BARE VERTEX

A starting point for the LKF transformations is knowledge of the Green's functions, here the FP, in the Landau gauge. We begin this study using the rainbow approximation (where the vertex is bare) since in this simple case the Landau gauge FP is easy to find. The well known SDE for the FP in quenched QED3 in the Minkowski space is :

$$S_M^{-1}(p; \xi) = S_M^{0-1}(p) - ie^2 \int \frac{d^3 k}{(2\pi)^3} \Gamma_M^\nu(k, p) S_M(k; \xi) \gamma^\mu \Delta_{\mu\nu}^{M0}(q), \quad (1)$$

where $q = k - p$ and e is the dimensionful electromagnetic coupling. The bare fermion and photon propagators, respectively, are $S_M^0(p) = 1/\not{p}$, $\Delta_{\mu\nu}^{M0}(q) = -g_{\mu\nu}/q^2 + (1 - \xi)q_\mu q_\nu/q^4$ and ξ is the covariant gauge parameter. $\Gamma_M^\mu(k, p)$ is the full fermion-boson vertex which we take to be bare, i.e., γ^μ , for the time being. We shall undo this assumption in Sect. V. and implement the full vertex. We prefer to write the FP in its most general form as $S_M(p; \xi) = F(p; \xi)/(\not{p} - \mathcal{M}(p; \xi))$. $F(p; \xi)$ is referred to as the wavefunction renormalization and $\mathcal{M}(p; \xi)$ as the mass function. The subscript M stands for the Minkowski space. Eq. (1) is a matrix equation. On multiplying it by 1 and \not{p} and taking the trace, it decomposes into a pair of coupled equations involving $F(p; \xi)$ and $\mathcal{M}(p; \xi)$. After a Wick rotation to Euclidean space, and performing angular integration, it is a common practice to write these equations as :

$$\frac{1}{F(p; \xi)} = 1 - \frac{\alpha\xi}{\pi p^2} \int dk \frac{k^2 F(k; \xi)}{k^2 + \mathcal{M}^2(k; \xi)} \left[1 - \frac{k^2 + p^2}{2kp} \ln \left| \frac{k+p}{k-p} \right| \right],$$

$$\frac{\mathcal{M}(p; \xi)}{F(p; \xi)} = \frac{\alpha(\xi + 2)}{\pi p} \int dk \frac{k F(k; \xi) \mathcal{M}(k; \xi)}{k^2 + \mathcal{M}^2(k; \xi)} \ln \left| \frac{k+p}{k-p} \right|,$$

where $\alpha = e^2/4\pi$. Owing to the fact that in the Landau gauge, $F(p; 0) = 1$, it has long served as a favourite gauge where one only has to solve the following equation :

$$\mathcal{M}(p; 0) = \frac{2\alpha}{\pi p} \int_0^\infty dk \frac{k \mathcal{M}(k; 0)}{k^2 + \mathcal{M}^2(k; 0)} \ln \left| \frac{k+p}{k-p} \right|. \quad (2)$$

The dynamically generated non perturbative solution of this equation is depicted as a solid line in Fig. (1). It corresponds to the appearance of masses through self interactions. In this article, we shall apply LKFT on this dynamically generated solution to find the result in an arbitrary covariant gauge. As we are interested in the analytical insight alone for the time being, we try to represent the solution of the FP in the Landau gauge with some simple analytical function. We note that for small momenta p , the solution for the mass function is roughly a constant. The large- p behaviour of the mass function can be studied by transforming Eq. (2) into a differential equation with the appropriate boundary conditions [12]. Note that in the integrand we can use the approximation $\ln |(k+p)/(k-p)| = (2p/k)\theta(k-p) + (2k/p)\theta(p-k)$, which is valid for $k \gg p$ and also for $k \ll p$. Substituting this expression into Eq. (2), we can re-write it in differential form as (we have rescaled the integral so that the corresponding solution of the differential equation can be expressed in units of e^4):

$$\frac{d}{dp} \left[p^3 \frac{d\mathcal{M}(p; 0)}{dp} \right] + \frac{2}{\pi^2} \mathcal{M}(p; 0) = 0, \quad (3)$$

with boundary conditions $p^3 d\mathcal{M}(p; 0)/dp = 0|_{p=0}$ and $\mathcal{M}(p; 0) = 0|_{p \rightarrow \infty}$. The solution of this equation is

$$\mathcal{M}(p; 0) = \frac{4}{\pi^2 p} \left[c_1 J_2 \left(\sqrt{\frac{8}{\pi^2 p}} \right) - c_2 Y_2 \left(\sqrt{\frac{8}{\pi^2 p}} \right) \right], \quad (4)$$

where $J(x)$ and $Y(x)$ are the Bessel functions of the first and second kind, respectively. The second boundary condition imposes $c_2 = 0$. As $J(1/\sqrt{p}) \rightarrow 1/p$ when $p \rightarrow \infty$, we conclude that $\mathcal{M}(p; 0) \rightarrow 1/p^2$ in this limit. The same conclusion is reached from the exact result, Fig. (1), by noticing that in the numerical data, $p^2 \mathcal{M}(p; 0)$ is practically constant near the upper end of the momentum region under consideration, namely, 10^3 . Therefore, we approximate the numerical solution by the following function :

$$\mathcal{M}(p; 0) = \frac{M_0 m_0^2}{p^2 + m_0^2}. \quad (5)$$

The numerical result suggests us to choose $M_0 = 0.10406$ and $m_0 = 0.1$ in order that the infrared and ultraviolet behaviour of the mass function are correctly reproduced. With this approximation, we find that the resulting Fourier transforms involved in LKFT (as we shall see later) are still not trivial to perform. Therefore, we need a further simplification. Owing to the fact that the mass function has the following infrared and ultraviolet features :

- region I : $p \ll m_0$

$$\mathcal{M}_I(p; 0) = M_0, \quad (6)$$

- region II : $p \gg m_0$

$$\mathcal{M}_{II}(p; 0) = \frac{M_0 m_0^2}{p^2}, \quad (7)$$

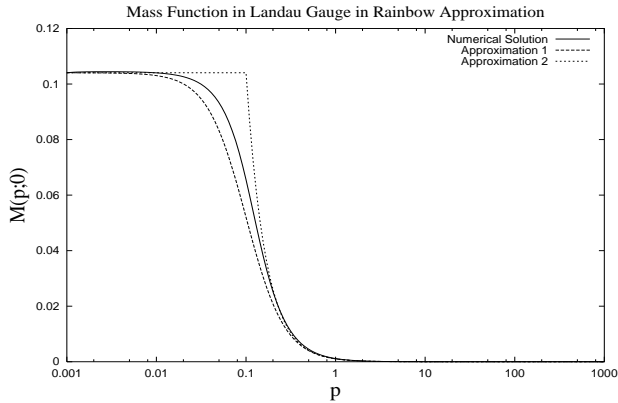


FIG. 1: The mass function in the Landau gauge for the bare vertex. Approximations proposed in Eq. (5) and Eq. (8) are also shown.

we can re-write the approximation to the mass function as follows :

$$\mathcal{M}(p;0) = M_0 \left[\theta(m_0 - p) + \frac{m_0^2}{p^2} \theta(p - m_0) \right]. \quad (8)$$

As shown in Fig. (1), Eqs. (5,8) provide a good approximation to the mass function in the infrared and ultraviolet regions. We are now in a position to apply the LKFT to this approximate solution to find the corresponding result in an arbitrary covariant gauge. We carry out this exercise in the next section.

III. LKFT AND THE DYNAMICALLY GENERATED MASS

We start by putting forward the definitions and notations we shall use along the way. We write out the FP in momentum and coordinate spaces, respectively, in its most general form as :

$$S_E(p; \xi) = A(p; \xi) + i \frac{B(p; \xi)}{\not{p}} \equiv \frac{F(p; \xi)}{i \not{p} - \mathcal{M}(p; \xi)}, \quad (9)$$

$$S_E(x; \xi) = \not{x} X(x; \xi) + Y(x; \xi), \quad (10)$$

The subscript E stands for the Euclidean space. The above expressions are related through the following Fourier transformations

$$S_E(p; \xi) = \int d^3x e^{ip \cdot x} S_E(x; \xi), \quad (11)$$

$$S_E(x; \xi) = \int \frac{d^3p}{(2\pi)^3} e^{-ip \cdot x} S_E(p; \xi). \quad (12)$$

The LKFT relating the coordinate space FP in Landau gauge to one in an arbitrary covariant gauge reads

$$S_E(x; \xi) = S_E(x; 0) e^{-ax}, \quad (13)$$

where $a = \alpha\xi/2$. The way we proceed is as follows : We start with a dynamically generated solution of the SDE for the FP in the Landau gauge and Fourier transform it to coordinate space. We then apply the LKFT law. Fourier transform of this result back to the momentum space yields the FP in an arbitrary covariant gauge.

A. Fermion Propagator in an Arbitrary Gauge in the Coordinate Space

As we have seen in section II that in the Landau gauge in the rainbow approximation, the function $F(p;0) = 1$. Therefore, the FP can be written $S_E(p;0) = 1/(i \not{p} - \mathcal{M}(p;0))$. Making use of this expression in Eqs. (10,12), the coordinate space FP in the Landau gauge can be written as :

$$X(x;0) = \frac{1}{2\pi^2 x^2} \int_0^\infty \frac{dp p^2}{p^2 + \mathcal{M}^2(p;0)} \left[\cos px - \frac{\sin px}{px} \right], \quad (14)$$

$$Y(x;0) = -\frac{1}{2\pi^2} \int_0^\infty \frac{dp p^2 \mathcal{M}(p;0)}{p^2 + \mathcal{M}^2(p;0)} \left[\frac{\sin px}{px} \right]. \quad (15)$$

For $\mathcal{M}(p;0)$, we shall use the approximate solution given in Eq. (8). It naturally divides the integration region in Eqs. (14,15) into two parts. Therefore,

$$X(x;0) = X_I + X_{II} \quad \text{and} \quad Y(x;0) = Y_I + Y_{II}, \quad (16)$$

where

$$X_I = \frac{1}{2\pi^2 x^2} \int_0^{m_0} \frac{dp p^2}{p^2 + M_0^2} \left[\cos px - \frac{\sin px}{px} \right], \quad (17)$$

$$X_{II} = \frac{1}{2\pi^2 x^2} \int_{m_0}^\infty \frac{dp p^6}{p^6 + M_0^2 m_0^4} \left[\cos px - \frac{\sin px}{px} \right], \quad (18)$$

$$Y_I = -\frac{1}{2\pi^2} \int_0^{m_0} \frac{dp p^2 M_0}{p^2 + M_0^2} \left[\frac{\sin px}{px} \right], \quad (19)$$

$$Y_{II} = -\frac{1}{2\pi^2} \int_{m_0}^\infty \frac{dp p^4 M_0 m_0^2}{p^6 + M_0^2 m_0^4} \left[\frac{\sin px}{px} \right]. \quad (20)$$

In order to be consistent with the approximations, Eqs. (6,7) made to arrive at Eq. (8), we neglect the corresponding terms in the denominators of the Eqs. (17-20), depending upon the region of integration over the momentum space. Thus carrying out the radial integrations, we obtain

$$\begin{aligned} X_I &= \frac{1}{2\pi^2 M_0^2 x^5} [3m_0 x \cos m_0 x + (m_0^2 x^2 - 3) \sin m_0 x], \\ X_{II} &= -\frac{1}{4\pi^2 x^3} [\pi + 2 \sin m_0 x - 2Si(m_0 x)], \\ Y_I &= \frac{m_0}{2\pi^2 M_0 x^2} \left[\cos m_0 x - \frac{\sin m_0 x}{m_0 x} \right], \\ Y_{II} &= -\frac{M_0 m_0}{4\pi^2} \left[\cos m_0 x + \frac{\sin m_0 x}{m_0 x} \right] \\ &\quad + \frac{M_0 m_0^2 x}{4\pi^2} \left[\frac{\pi}{2} - Si(m_0 x) \right], \end{aligned} \quad (21)$$

where $Si(y)$ is the Sine Integral function, given by :

$$Si(y) = \int_0^y \frac{\sin t}{t} dt. \quad (22)$$

Now Eqs. (10,13,16-21) constitute the FP in an arbitrary covariant gauge in the coordinate space. In the next section, we Fourier transform this result back to the momentum space.

B. Fermion Propagator in an Arbitrary Gauge in the Momentum Space

In order to carry out the inverse Fourier transform, we use the auxiliary functions $A(p; \xi)$ and $B(p; \xi)$ which are related to the more familiar functions $\mathcal{M}(p; \xi)$ and $F(p; \xi)$ in a simple fashion :

$$\mathcal{M}(p; \xi) = p^2 \frac{A(p; \xi)}{B(p; \xi)}, \quad (23)$$

$$F(p; \xi) = -B(p; \xi) - p^2 \frac{A^2(p; \xi)}{B(p; \xi)}. \quad (24)$$

In terms of $X(x; \xi)$ and $Y(x; \xi)$, the auxiliary functions can be written as follows :

$$\begin{aligned} A(p; \xi) &= \int d^3x e^{ip \cdot x} Y(x; \xi) \\ &= \frac{4\pi}{p} \int_0^\infty dx x \sin px Y(x; \xi), \end{aligned} \quad (25)$$

$$\begin{aligned} B(p; \xi) &= \frac{1}{i} \int d^3x p \cdot x e^{ip \cdot x} X(x; \xi) \\ &= 4\pi \int_0^\infty dx x^2 \left[\frac{\sin px}{px} - \cos px \right] X(x; \xi). \end{aligned} \quad (26)$$

We shall eventually be interested in the large and small limits of the momentum as compared to the dynamically generated mass scale m_0 . However, as the coupling also has mass dimensions, special care may be needed for the evaluation of the the above integrals, especially for the B -term as we shall shortly see. We evaluate the A -term and the B -term separately below.

1. The A -term

Making use of Eqs. (16-21), $A(p; \xi)$ can be expanded term by term as :

$$\begin{aligned} A(p; \xi) &= \frac{2m_0}{\pi M_0 p} A_1(p; \xi) - \frac{M_0 m_0}{\pi p} A_2(p; \xi) \\ &+ \frac{M_0 m_0^2}{\pi p} A_3(p; \xi), \end{aligned} \quad (27)$$

where

$$A_1(p; \xi) = \int_0^\infty \frac{dx}{x} e^{-ax} \sin px \left[\cos m_0 x - \frac{\sin m_0 x}{m_0 x} \right]$$

$$\begin{aligned} A_2(p; \xi) &= \int_0^\infty dx x e^{-ax} \sin px \left[\cos m_0 x + \frac{\sin m_0 x}{m_0 x} \right] \\ A_3(p; \xi) &= \int_0^\infty dx x^2 e^{-ax} \sin px \left[\frac{\pi}{2} - Si(m_0 x) \right]. \end{aligned} \quad (28)$$

The results of these integrations have been presented in the appendix. The addition and simplification of these expressions brings about some cancellations to yield the final simple result as :

$$\begin{aligned} A(p; \xi) &= -\frac{1}{\pi} \left[\frac{1}{M_0} + \frac{M_0 m_0^2 (3a^2 - p^2)}{(a^2 + p^2)^3} \right] [T_+ + T_-] \\ &+ \frac{a}{2\pi p} \left[\frac{1}{M_0} - \frac{M_0 m_0^2 (a^2 - 3p^2)}{(a^2 + p^2)^3} \right] L \\ &+ \frac{M_0 m_0}{(a^2 + p^2)^2} \left[-\frac{4a}{\pi} + m_0 \frac{(3a^2 - p^2)}{a^2 + p^2} \right], \end{aligned} \quad (29)$$

where

$$\begin{aligned} T_\pm &= \arctan \left[\frac{m_0 \pm p}{a} \right], \\ L &= \ln \left| \frac{a^2 + (m_0 + p)^2}{a^2 + (m_0 - p)^2} \right|. \end{aligned} \quad (30)$$

2. The B -term

We carry out a similar procedure to evaluate $B(p, \xi)$. However, the integrations involved are harder as we shall shortly see. Eqs. (16-21) permit us to write

$$\begin{aligned} B(p, \xi) &= -\frac{6m_0}{\pi M_0^2} B_1(p; \xi) + \frac{2}{\pi} \left[1 - \frac{m_0^2}{M_0^2} \right] B_2(p; \xi) \\ &+ B_3(p; \xi) - \frac{2}{\pi} B_4(p; \xi), \end{aligned} \quad (31)$$

where the integrals involved are outlined below :

$$\begin{aligned} B_1(p; \xi) &= \int_0^\infty \frac{dx}{x^2} e^{-ax} \left[\cos m_0 x - \frac{\sin m_0 x}{m_0 x} \right] \\ &\quad \left[\cos px - \frac{\sin px}{px} \right] \\ B_2(p; \xi) &= \int_0^\infty \frac{dx}{x} e^{-ax} \sin m_0 x \left[\cos px - \frac{\sin px}{px} \right] \\ B_3(p; \xi) &= \int_0^\infty \frac{dx}{x} e^{-ax} \left[\cos px - \frac{\sin px}{px} \right] \\ B_4(p; \xi) &= \int_0^\infty \frac{dx}{x} e^{-ax} \left[\cos px - \frac{\sin px}{px} \right] Si(m_0 x). \end{aligned} \quad (32)$$

Except the last one, the other integrals are less complicated to evaluate. Making use of the same notations as before, these are listed below :

$$\begin{aligned} B_1(p; \xi) &= \frac{1}{6m_0 p} [(m_0^3 + p^3)T_+ - (m_0^3 - p^3)T_-] \\ &+ \frac{a}{24m_0 p} [4m_0 p + (a^2 + 3m_0^2 + 3p^3)L] \end{aligned}$$

$$\begin{aligned}
B_2(p; \xi) &= \frac{m_0}{2p} [T_- - T_+] - \frac{a}{4p} L \\
B_3(p; \xi) &= -1 + \frac{a}{p} \arctan \frac{p}{a}.
\end{aligned} \tag{33}$$

A word of caution is appropriate here. In order to verify our findings, we shall always want to make a connection of our results for the large and small values of momentum to the ones in the Landau gauge. It appears that B_3 may offer a tricky problem in this context because after taking the small p limit, we cannot retreat to the Landau gauge which corresponds to the $a \rightarrow 0$ limit. The term $B_4(p; \xi)$ comes to our rescue and it becomes evident if treated carefully. It is for this reason that we prefer to write it in the form :

$$B_4(p; \xi) = \sum_{n=0}^{\infty} (-1)^n \frac{a^n}{n!} I_n, \tag{34}$$

where

$$I_n = \int_0^{\infty} dx x^{n-1} \left[\cos px - \frac{\sin px}{px} \right] Si(m_0 x). \tag{35}$$

This expression is perhaps the most convenient to deduce the FP for the asymptotic limits of momenta and then also to be able to make connection with the results of the Landau gauge. One can find out that when $m_0 < p$,

$$\begin{aligned}
I_n &= -\frac{m_0}{p^{1+n}} \times \\
&\left[\Gamma(1+n) {}_pF_q \left[\left\{ \frac{1}{2}, \frac{n+1}{2}, 1 + \frac{n}{2} \right\}, \left\{ \frac{3}{2}, \frac{3}{2} \right\}; \frac{m_0^2}{p^2} \right] \right. \\
&\left. + \Gamma(n) {}_pF_q \left[\left\{ \frac{1}{2}, \frac{n+1}{2}, \frac{n}{2} \right\}, \left\{ \frac{3}{2}, \frac{3}{2} \right\}; \frac{m_0^2}{p^2} \right] \right], \tag{36}
\end{aligned}$$

and when $m_0 > p$

$$\begin{aligned}
I_n &= \frac{\pi}{2p^n} \cos \left(\frac{n\pi}{2} \right) [\Gamma(n-1) + \Gamma(n)] + \frac{\Gamma(n)}{nm_0^n} \sin \left(\frac{n\pi}{2} \right) \\
&\times \left[- {}_pF_q \left[\left\{ \frac{n+1}{2}, \frac{n}{2}, \frac{n}{2} \right\}, \left\{ \frac{1}{2}, 1 + \frac{n}{2} \right\}; \frac{p^2}{m_0^2} \right] \right. \\
&\left. + {}_pF_q \left[\left\{ \frac{n+1}{2}, \frac{n}{2}, \frac{n}{2} \right\}, \left\{ \frac{3}{2}, 1 + \frac{n}{2} \right\}; \frac{p^2}{m_0^2} \right] \right]. \tag{37}
\end{aligned}$$

Finally, Eqs. (9,29-37) give the dynamically generated FP in an arbitrary covariant gauge.

IV. RELEVANT LIMITS

We are now in a position to carry out the analytic analysis of the results obtained in the previous section. We analyse dynamically generated FP in the asymptotic limits of momenta, i.e., when $p \gg m_0$ and $m_0 \gg p$.

In order to make a quick comparison possible, we write below the expressions for $A(p; 0)$ and $B(p; 0)$:

$$A(p; 0) = -\frac{1}{M_0} \left[\theta(m_0 - p) + \frac{M_0^2 m_0^2}{p^4} \theta(p - m_0) \right], \tag{38}$$

$$B(p; 0) = -\left[\frac{p^2}{M_0^4} \theta(m_0 - p) + \theta(p - m_0) \right]. \tag{39}$$

We now proceed to evaluate the asymptotic limits of the LKF transformed functions.

A. Large- p Behaviour of the Fermion Propagator

In the large- p limit, one can verify that

$$\begin{aligned}
A(p; \xi) &= \left[-m_0^2 M_0 - \frac{4am_0(m_0^2 + 3M_0^2)}{3M_0\pi} \right] \frac{1}{p^4} \\
&\quad + \mathcal{O} \left(\frac{1}{p^6} \right),
\end{aligned} \tag{40}$$

$$B(p; \xi) = -1 + \mathcal{O} \left(\frac{1}{p} \right). \tag{41}$$

The Landau gauge results, Eqs. (38,39), are readily reproduced if we substitute $a = 0$. Correspondingly, the mass function and the wavefunction renormalization acquire the following form :

$$\begin{aligned}
\mathcal{M}(p; \xi) &= \left[m_0^2 M_0 + \frac{4am_0(m_0^2 + 3M_0^2)}{3M_0\pi} \right] \frac{1}{p^2} + \mathcal{O} \left(\frac{1}{p^3} \right) \\
&\equiv \frac{C_3(\xi)}{p^2} + \mathcal{O} \left(\frac{1}{p^3} \right),
\end{aligned} \tag{42}$$

$$F(p; \xi) = 1 + \mathcal{O} \left(\frac{1}{p} \right). \tag{43}$$

Again, obviously, if we set $a = 0$, we recover the Landau gauge results. An important implication of these last equations is that in an arbitrary covariant gauge, the mass function will continue to fall as $1/p^2$ for its asymptotically large values. Numerically, such an effect was seen although for a very small range of values of the gauge parameter ($\xi = 0 - 1$) in [9]. For a much broader range ($\xi = 0 - 5$), the same observation was reported in [10]. Here, the analytical incorporation of the LKFT allows us to generalise these findings to an arbitrarily large value of the gauge parameter. Moreover, the wavefunction renormalization continues to approach 1 in the large p limit for arbitrarily large values of the gauge parameter. This fact is also in accordance with the numerical computations done for a limited range of ξ [9, 10].

B. Low- p Behaviour of the Fermion Propagator

An analogous analysis for the low- p regime yields

$$A(p; \xi) = \left[\frac{m_0 M_0}{a^4} \left(3m_0 - \frac{4a}{\pi} \right) \right]$$

$$\begin{aligned}
& + \frac{2am_0}{\pi(a^2 + m_0^2)} \left(\frac{1}{M_0} - \frac{m_0^2 M_0}{a^4} \right) \\
& - \frac{2}{\pi} \left(\frac{1}{M_0} + \frac{3m_0^2 M_0}{a^4} \right) \arctan \frac{m_0}{a} \Big] + \mathcal{O}(p^2) \\
\equiv & C_1(\xi) + \mathcal{O}(p^2), \tag{44}
\end{aligned}$$

$$\begin{aligned}
B(p; \xi) &= \frac{2}{3M_0^2 \pi} \left[\frac{am_0(3a^2 + 5m_0^2 - 2M_0^2)}{(a^2 + m_0^2)^2} \right. \\
& \quad \left. - 3 \arctan \frac{m_0}{a} \right] p^2 + \mathcal{O}(p^3) \\
\equiv & C_2(\xi) p^2 + \mathcal{O}(p^3), \tag{45}
\end{aligned}$$

where a neat cancellation has taken place between B_3 and the first sum in B_4 (refer to the last equation of the Appendix). Taking the limit $a \rightarrow 0$, we again recuperate the corresponding results in Eqs. (38,39). The mass function and the wavefunction renormalization can now be calculated to be :

$$\mathcal{M}(p; \xi) = \frac{C_1(\xi)}{C_2(\xi)} + \mathcal{O}(p^2), \tag{46}$$

$$F(p; \xi) = -\frac{C_1^2(\xi)}{C_2(\xi)} - C_2(\xi)p^2 + \mathcal{O}(p^4). \tag{47}$$

Expectedly,

- The mass function is flat for small values of p , and it falls off as $1/p^2$ for its large values. This behaviour was observed for a very limited number of values of ξ in [9, 10] after a complicated numerical exercise. Here we prove it to be the case analytically *in an arbitrary covariant gauge*.
- The wavefunction renormalization is also a constant for small values of p . For the large values, it approaches 1. This fact is not a feature of $F(p^2)$ just in the neighbourhood of the Landau gauge. It is true independent of our selection of ξ .

Thus the p -dependence of the dynamically generated FP for the small and large values of the momentum continues to have the same qualitative features in an arbitrary covariant gauge as the ones in the Landau gauge and in its neighbourhood, [9, 10].

V. FULL VERTEX

In the previous sections, we have relied on the assumption that the bare vertex is the correct approximation in the Landau gauge. Several works indicate that this is not the case. The latest in a series of proposals for the full vertex in QED3 is the one suggested in [6]. However, its employment to solve the SDE for the FP is a formidable task even in the Landau gauge. In perturbation theory, as indicated in [13] (see Eq. (26) of that article), the transverse vertex in fact vanishes in the Landau gauge

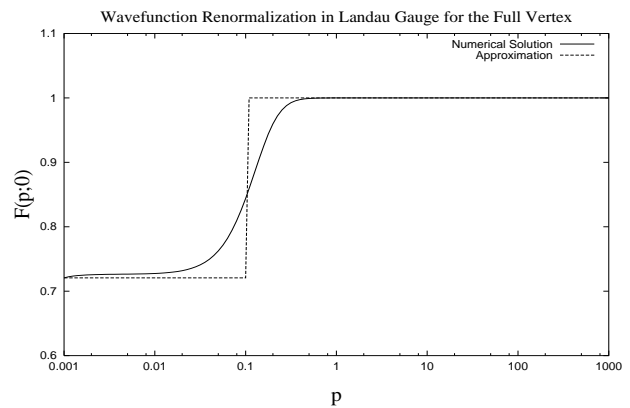


FIG. 2: Wavefunction Renormalization in the Landau gauge for the full vertex. Approximation proposed in Eq. (48) is also shown.

in the limit $k^2 \gg p^2$ for QED in arbitrary dimensions. Based upon this, there are several suggestions of using a full vertex whose transverse part vanishes in the Landau gauge. In this article, we concentrate on all such vertices, e.g., [14, 15, 16, 17]. In this case, the numerical behaviour of the wavefunction renormalization modifies to the one shown in Fig. (2). It is no longer 1 for all momentum regimes. Instead, it behaves like a constant (different from unity) for low momentum, and tends to one as $p \rightarrow \infty$. Therefore, in addition to using the approximation in Eq. (8) for the mass function (with M_0 replaced by M_{0F} and m_0 by m_{0F} because the solutions in the Landau gauge for the bare vertex and the full vertex are not identical), we can use the following simple form for the wavefunction renormalization in the Landau gauge, Fig. (2) :

$$F(p, 0) = F_{0F} \theta(m_{0F} - p) + \theta(p - m_{0F}). \tag{48}$$

Following the steps outlined earlier, it is easy to notice that only the terms X_I and Y_I get multiplied by the constant factor F_0 , whereas, the rest remains unchanged. This fact makes the LKFT exercise straightforward. The slight modifications to the $A(p; \xi)$ and $B(p; \xi)$ terms are the following :

$$\begin{aligned}
A(p; \xi) &= -\frac{1}{\pi} \left[\frac{F_{0F}}{M_{0F}} + \frac{M_{0F} m_{0F}^2 (3a^2 - p^2)}{(a^2 + p^2)^3} \right] [T_+ + T_-] \\
&+ \frac{a}{2\pi p} \left[\frac{F_{0F}}{M_{0F}} - \frac{M_{0F} m_{0F}^2 (a^2 - 3p^2)}{(a^2 + p^2)^3} \right] L \\
&+ \frac{M_{0F} m_{0F}}{(a^2 + p^2)^2} \left[-\frac{4a}{\pi} + m_{0F} \frac{(3a^2 - p^2)}{a^2 + p^2} \right] \tag{49}
\end{aligned}$$

$$\begin{aligned}
B(p, \xi) &= -\frac{6m_{0F} F_{0F}}{\pi M_{0F}^2} B_1 + \frac{2}{\pi} \left[1 - \frac{m_{0F}^2 F_{0F}}{M_{0F}^2} \right] B_2 \\
&+ B_3 - \frac{2}{\pi} B_4, \tag{50}
\end{aligned}$$

where B_1, B_2, B_3 and B_4 have been already calculated. The large momentum limit for these expressions is now

$$A(p; \xi) = \left[-m_{0F}^2 M_{0F} - \frac{4am_{0F}(m_{0F}^2 F_{0F} + 3M_{0F}^2)}{3M_{0F}\pi} \right] \frac{1}{p^4} + \mathcal{O}\left(\frac{1}{p^6}\right), \quad (51)$$

$$B(p; \xi) = -1 + \mathcal{O}\left(\frac{1}{p}\right). \quad (52)$$

Consequently,

$$\begin{aligned} \mathcal{M}(p; \xi) &= \left[m_{0F}^2 M_{0F} + \frac{4am_{0F}(m_{0F}^2 F_{0F} + 3M_{0F}^2)}{3M_{0F}\pi} \right] \frac{1}{p^2} \\ &+ \mathcal{O}\left(\frac{1}{p^3}\right) \\ &\equiv \frac{C_{3F}(\xi)}{p^2} + \mathcal{O}\left(\frac{1}{p^3}\right), \end{aligned} \quad (53)$$

$$F(p; \xi) = 1 + \mathcal{O}\left(\frac{1}{p}\right). \quad (54)$$

In a similar fashion, for the low- p behaviour, we now arrive at the following expressions for $A(p; \xi)$ and $B(p; \xi)$

$$\begin{aligned} A(p; \xi) &= \left[\frac{m_{0F} M_{0F}}{a^4} \left(3m_{0F} - \frac{4a}{\pi} \right) \right. \\ &+ \frac{2am_{0F}}{\pi(a^2 + m_{0F}^2)} \left(\frac{F_{0F}}{M_{0F}} - \frac{m_{0F}^2 M_{0F}}{a^4} \right) \\ &- \left. \frac{2}{\pi} \left(\frac{F_{0F}}{M_{0F}} + \frac{3m_{0F}^2 M_{0F}}{a^4} \right) \arctan \frac{m_{0F}}{a} \right] \\ &+ \mathcal{O}(p^2) \\ &\equiv C_{1F}(\xi) + \mathcal{O}(p^2), \end{aligned} \quad (55)$$

$$\begin{aligned} B(p; \xi) &= \frac{2}{3M_{0F}^2 \pi} \left[\frac{am_{0F}(3a^2 F_{0F} + 5m_{0F}^2 F_{0F} - 2M_{0F}^2)}{(a^2 + m_{0F}^2)^2} \right. \\ &- \left. 3F_{0F} \arctan \frac{m_{0F}}{a} \right] p^2 + \mathcal{O}(p^3) \\ &\equiv C_{2F}(\xi) p^2 + \mathcal{O}(p^3). \end{aligned} \quad (56)$$

These functions easily get translated into the more familiar functions $F(p; \xi)$ and $\mathcal{M}(p; \xi)$

$$\mathcal{M}(p; \xi) = \frac{C_{1F}(\xi)}{C_{2F}(\xi)} + \mathcal{O}(p^2), \quad (57)$$

$$F(p; \xi) = -\frac{C_{1F}^2(\xi)}{C_{2F}(\xi)} - C_{2F}(\xi) p^2 + \mathcal{O}(p^4). \quad (58)$$

We note that the incorporation of the full vertex does not change the qualitative features of the mass function and the wavefunction renormalization. The mass function is flat in the infrared limit and falls off as $1/p^2$ in the ultraviolet region. The wavefunction renormalization is also a constant for low values of p . It approaches 1 as

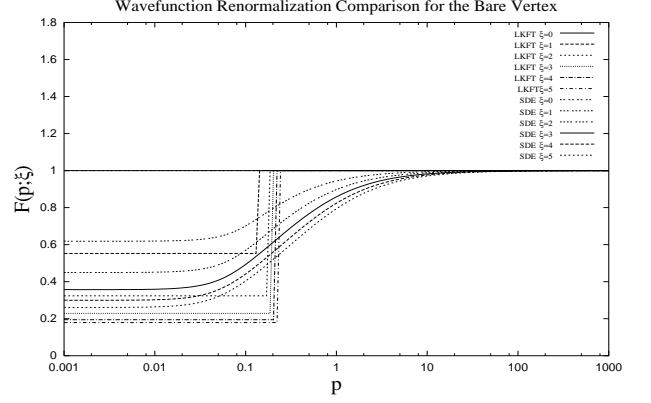


FIG. 3: Wavefunction renormalization for the bare vertex employing LKFT. For a comparison, we also plot the results obtained by directly solving SDE.

momentum p acquires large values. However, the constants multiplying these solutions get modified on employing the full vertex. To get a quantitative estimate of this modification we carry out a numerical exercise in the next section.

VI. NUMERICAL FINDINGS

As stressed before, we cannot expect the numerical results presented in this section to be quantitatively exact and a true reflection of the choice of the full vertex owing to the facts that (i) the Landau gauge result has been approximated by a simple analytic function, and (ii) approximations (6,7) have been employed in order to ensure that an analytical insight could be obtained. However, the approximate results indicate that we are making progress in the right direction.

In order to view graphically our numerical results, we proceed as follows. From the corresponding expressions in the low and large momentum regimes for F and \mathcal{M} , we perform the following parametrisation for the FP in arbitrary gauge :

$$\mathcal{M}(p; \xi) = M_{\xi(F)} \left[\theta(m_{\xi(F)} - p) + \frac{m_{\xi(F)}^2}{p^2} \theta(p - m_{\xi(F)}) \right] \quad (59)$$

$$F(p; \xi) = F_{\xi(F)} \theta(m_{\xi(F)} - p) + \theta(p - m_{\xi(F)}), \quad (60)$$

where

$$\begin{aligned} M_{\xi(F)} &= \frac{C_{1(F)}(\xi)}{C_{2(F)}(\xi)} \\ M_{\xi(F)} m_{\xi(F)}^2 &= C_{3(F)}(\xi) \\ F_{\xi(F)} &= -\frac{C_{1(F)}^2(\xi)}{C_{2(F)}(\xi)}. \end{aligned}$$

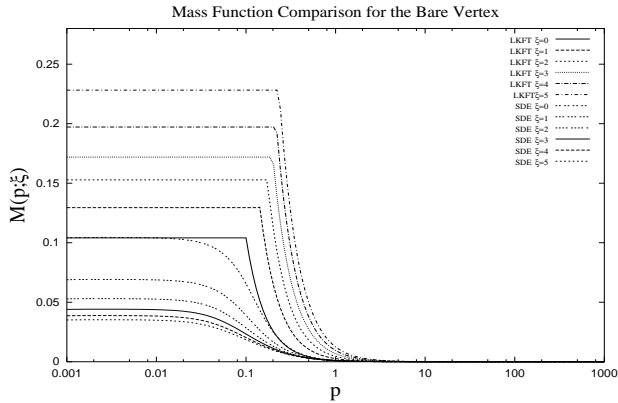


FIG. 4: Mass function for the bare vertex employing LKFT. For a comparison, we also plot the results obtained by directly solving SDE.

and note that it obviously reduces to (8) and (48) on setting $\xi = 0$. We separate the discussion on the bare and the full vertex in the following subsections.

A. Bare Vertex

- In Fig. (3), we have plotted the wavefunction renormalization in various gauges. Comparing them with the ones obtained by solving SDE, one sees that the difference is not enormous, reassuring the correctness of the method employed.
- In Fig. (4), we have plotted the mass function in several gauges in order to compare the results of directly solving SDE against the ones obtained by employing the LKFT. With the increasing value of the gauge parameter, the direction of the shift in the mass function is diametrically opposed for both the cases. Which one should we trust more? LKFT arise as a necessary condition of gauge invariance. Therefore, one would naturally regard the results more plausible after these transformations have been taken into account. We shall see later that the studies carried out by including the full vertex justify this argument.

B. Full Vertex

SDE for the FP will yield an exact result if a full vertex is employed which complies with *all* the constraints imposed on it by the corresponding gauge field theory. Construction and usage of such a vertex is a prohibitively difficult task. Following the works of Ball and Chiu, we can divide the full vertex into two parts, the longitudinal, which ensures WGTI is satisfied and the transverse which

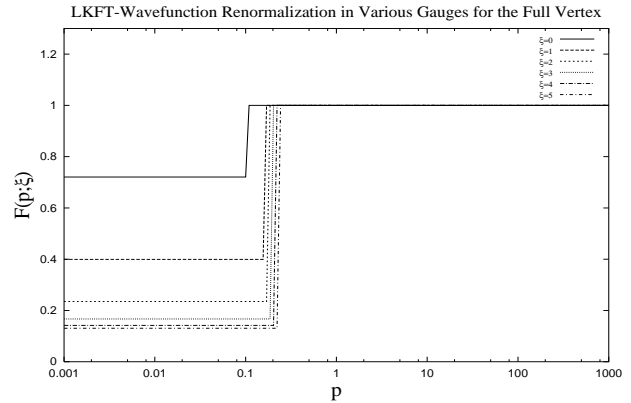


FIG. 5: Wave function renormalization for the full vertex employing LKFT.

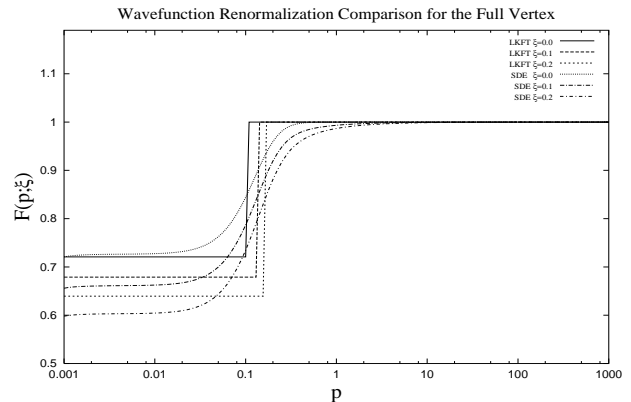


FIG. 6: A comparison of the results for the wavefunction renormalization (i) employing LKFT and (ii) results obtained by directly solving SDE for the full vertex.

vanishes on contraction with the photon momentum vector and remains undetermined by the WGTI. One of the most recent (and so far perhaps the most complete) attempts to propose such a vertex in quenched QED3 can be found in [6]. However, it is obviously a hard choice for its numerical implementation. For the purpose of being able to compare our results with earlier works we restrict ourselves to the family of transverse vertices which vanish in the Landau gauge although an extension to a more general case is straightforward. We observe the following:

- In Fig. (5), we have plotted the wavefunction renormalization in several gauges and in Fig. (6), we present a comparison against the results of directly solving SDEs. The results are found to be in fairly good agreement.
- In Fig. (7), we have plotted the mass function in several gauges. In case of the full vertex, it is a bit hard to compare the results of directly solving SDE

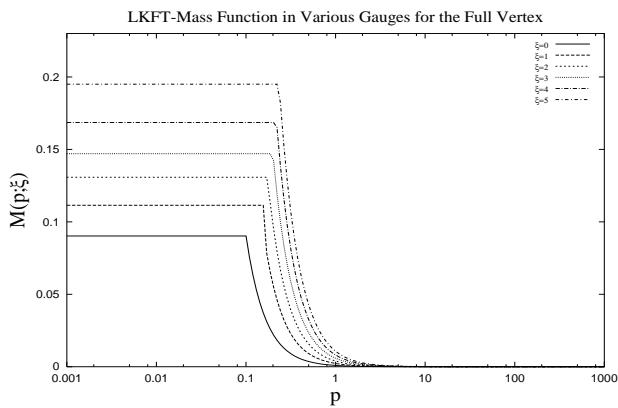


FIG. 7: Mass function for the full vertex employing LKFT.

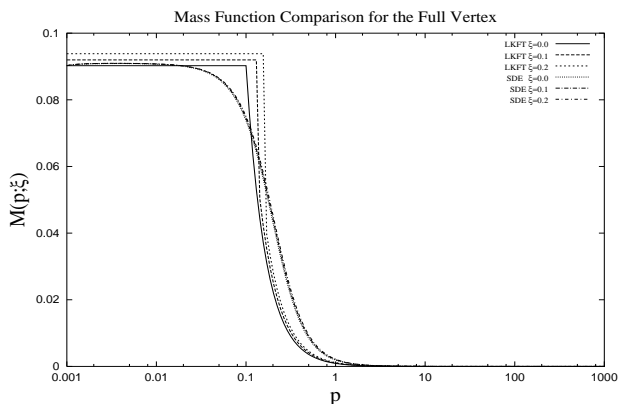


FIG. 8: A comparison of the results for the mass function (i) employing LKFT and (ii) results obtained by directly solving SDE for the full vertex.

against the ones obtained by employing the LKFT as the results in the former case are known only in a small region near the Landau gauge [9, 10, 18]. We offer a comparison in Fig. (8). An interesting thing we note is that in both the cases the trend for the function is to get shifted upwards with increasing values of the gauge parameter. This is the same behaviour as we had noted for the bare vertex by using the LKFT. Moreover, the difference between the two types of approaches seems to close down on each other when the full vertex is employed. It is understandable as the constraints of gauge invariance are now being used in both the cases. A considerable advantage of using LKFT method is that the results for an arbitrary value of the covariant gauge parameter are readily available.

VII. CONCLUSIONS

The bulk of strong interaction phenomena require a non-perturbative approach. An example is the dynamical generation of fundamental fermion masses, which lies beyond the realm of perturbation theory. This phenomenon is linked with the non-perturbative behaviour of the FP and is governed by its SDE. As the SDE of the higher point Green functions are intricately related to it, a meaningful truncation scheme which maintains the key features of the theory, such as gauge invariance, continues to be a challenging problem. Along with other guiding principles, a correct inclusion of the LKFT of the FP and the fermion-boson interaction is crucial for arriving at reliable conclusions. We carry out a preliminary study in this connection. Starting from a dynamically generated chirally asymmetric FP in one gauge, we perform an LKFT to find its form and properties in an arbitrary covariant gauge ξ . Encouragingly, we find expected behaviour of the FP for the asymptotic regimes of momenta for all ξ , a fact supported by earlier direct numerical solutions of the SDE (where no reference is made to the LKFT) in a small region of ξ close to the Landau gauge [9, 10]. The initial results for quenched QED3 presented here provide the starting point for a more rigorous and exact numerical study. One can then go on to take up the more interesting case of QED4. The solution to this problem will in turn be the starting point for a study of QCD where the non-abelian nature of interactions, so essential for both confinement and asymptotic freedom, will further complicate the problem. All this is for the future.

Acknowledgements: We wish to thank M. R. Pennington for suggesting the problem and to him and R. Delbourgo for their comments on the draft version of this article. We acknowledge CIC (project 4.12), CONACyT and Alvarez-Buylla grants.

Appendix

We list below several of the integrals used, [19], in this article for a quick reference. Fourier transforming the Landau gauge FP in the momentum space to the one in the coordinate space requires the following integrals :

$$\int_0^m dp p^2 \left[\cos px - \frac{\sin px}{px} \right] = \frac{3mx \cos mx}{x^3} + \frac{(m^2 x^2 - 3) \sin mx}{x^3}$$

$$\int_m^\infty dp \left[\cos px - \frac{\sin px}{px} \right] = -\frac{\pi + 2 \sin mx - 2Si(mx)}{2x}$$

$$\int_0^m dp p \sin px = \left[-\frac{m \cos mx}{x} + \frac{\sin mx}{x^2} \right]$$

$$\int_m^\infty \frac{dp}{p^3} \sin px = \frac{x}{2m} \left[\frac{\sin mx}{mx} + \cos mx \right] - \frac{x^2}{2} \left[\frac{\pi}{2} - Si(mx) \right].$$

The Fourier transform back to the momentum space after having performed the LKFT makes use of the following results :

$$\begin{aligned} A_1(p; \xi) &= -\frac{p}{2m_0} [T_+ + T_-] + \frac{aL}{4m_0} \\ A_2(p; \xi) &= \frac{-p[m_0^4 - (a^2 + p^2)^2]}{[a^2 + (m_0 - p)^2]^2 [a^2 + (m_0 + p)^2]^2} \\ A_3(p; \xi) &= -\frac{1}{(a^2 + p^2)^3} \left[p(3a^2 - p^2)(T_+ + T_- - \pi) \right. \\ &\quad \left. + (a^2 - 3p^2)L + \frac{4am_0p(a^2 + p^2)(2a^2 + m_0^2 - 2p^2)}{A_- A_+} \right. \\ &\quad \left. + a(a^2 + p^2)^2 \left\{ \frac{p(m_0 - p)}{A_-^2} + \frac{p(m_0 + p)}{A_+^2} \right. \right. \\ &\quad \left. \left. + \frac{a^2 - (m_0 - p)^2}{2A_-^2} - \frac{a^2 - (m_0 + p)^2}{2A_+^2} \right\} \right], \end{aligned}$$

where

$$A_{\pm} = a^2 + (m_0 \pm p)^2.$$

In arriving at the above relations, we have made use of the following relations

$$\begin{aligned} \int_0^\infty dx x^2 \sin(px) e^{-ax} &= 2p \frac{(3a^2 - p^2)}{(a^2 + p^2)^3} \\ \int_0^\infty \frac{dx}{x} e^{-ax} \sin m_0 x \cos px &= \frac{1}{2} [T_- + T_+] \\ \int_0^\infty dx e^{-ax} \sin m_0 x \cos px &= \frac{m_0(a^2 + m_0^2 - p^2)}{A_- A_+} \\ \int_0^\infty dx x e^{-ax} \sin m_0 x \cos px &= a \left[\frac{m_0 - p}{A_-^2} + \frac{m_0 + p}{A_+^2} \right] \\ \int_0^\infty \frac{dx}{x} e^{-ax} \sin m_0 x \sin px &= \frac{L}{4} \\ \int_0^\infty dx e^{-ax} \sin m_0 x \sin px &= \frac{2am_0p}{A_- A_+} \\ \int_0^\infty dx x e^{-ax} \sin m_0 x \sin px &= \frac{1}{2} \left[\frac{\cos 2T_-}{A_-} - \frac{\cos 2T_+}{A_+} \right]. \end{aligned}$$

We have also made use of the following sum

$$\sum_{n=0}^{\infty} \frac{(-a)^n}{n! p^n} \cos\left(\frac{n\pi}{2}\right) [\Gamma(n-1) + \Gamma(n)] = -1 + \frac{a}{p} \arctan \frac{p}{a}.$$

-
- [1] N. Dorey and N.E. Mavromatos, Nucl. Phys. **B386** 614 (1992); K. Farakos and N.E. Mavromatos, Mod. Phys. Lett. **A13** 1019 (1998); I.F. Herbut, Phys. Rev. **B66** 094512 (2002), M. Franz, Z. Tesanovic and O. Vafek, Phys. Rev. **B66** 054535 (2002).
- [2] S.J. Hands, J.B. Kogut and C.G. Strouthos, hep-lat/0404013; S.J. Hands, J.B. Kogut and C.G. Strouthos, Nucl. Phys. **B645** 321 (2002); S.J. Hands, J.B. Kogut, L. Scorzato and C.G. Strouthos, Nucl. Phys. Proc. Suppl. **119** 974 (2003); V.P. Gusynin and M. Reenders, Phys. Rev. **D68** 025017 (2003); M.R. Pennington and D. Walsh, Phys. Lett. **B253** 246 (1991).
- [3] J.C. Ward, Phys. Rev. **78** (1950); H.S. Green, Proc. Phys. Soc. (London) **A66** 873 (1953); Y. Takahashi, Nuovo Cimento **6** 371 (1957).
- [4] N.K. Nielsen, Nucl. Phys. **B101** 173 (1975); O. Piguet and K. Sibold, Nucl. Phys. **B253** 517 (1985).
- [5] L.D. Landau and I.M. Khalatnikov, Zh. Eksp. Teor. Fiz. **29** 89 (1956); L.D. Landau and I.M. Khalatnikov, Sov. Phys. JETP **2** 69 (1956); E.S. Fradkin, Sov. Phys. JETP **2** 361 (1956); K. Johnson and B. Zumino, Phys. Rev. Lett. **3** 351 (1959); B. Zumino, J. Math. Phys. **1** 1 (1960).
- [6] A. Bashir and A. Raya, Phys. Rev. **D64** 105001 (2001); A. Raya, *Gauge Invariance and Construction of the Fermion-Boson Vertex in QED3*, Ph. D. Thesis, Universidad Michoacana de San Nicolás de Hidalgo, México (2003).
- [7] R. Delbourgo and B.W. Keck, J. Phys. **A13** 701 (1980); R. Delbourgo, B.W. Keck and C.N. Parker, J. Phys. **A14** 921 (1981).
- [8] A. Bashir and A. Raya, Phys. Rev. **D66** 105005 (2002); A. Bashir, Phys. Lett. **B491** 280 (2000).
- [9] C.J. Burden and C.D. Roberts, Phys. Rev. **D44** 540 (1991).
- [10] A. Bashir, A. Huet and A. Raya, Phys. Rev. **D66** 025029 (2002).
- [11] A. Raya, "The fermion propagator in the light of its Landau-Khalatnikov-Fradkin transformation", talk given at the QCD Downunder Workshop, University of Adelaide, Adelaide, Australia (2004).
- [12] C.D. Roberts and A.G. Williams, Prog. Part. Nucl. Phys. **33** 477 (1994).
- [13] A. Bashir and R. Delbourgo, hep-ph/0405018.
- [14] J.S. Ball y T.-W. Chiu, Phys. Rev. **D22** 2542 (1980).
- [15] D.C. Curtis and M.R. Pennington, Phys. Rev. **D42** 4165 (1990).
- [16] A. Bashir and M.R. Pennington, Phys. Rev. **D50** 7679 (1994).
- [17] Z. Dong, H.J. Munczek and C.D. Roberts, Phys. Lett. **B333** 544 (1994).
- [18] A. Huet, *Numerical Analysis of the Schwinger-Dyson Equations*, M. Sc. Thesis, Universidad Michoacana de San Nicolás de Hidalgo, México (2003).
- [19] I.S. Gradshteyn and I.M. Ryzhik, *Table of Integrals, Series and Products, sixth edition*, (Academic Press, USA), (2000); M. Abramowitz and I.A. Stegun, *Handbook of Mathematical Functions, tenth printing*, (Dover Publications, USA), (1972); S. Wolfram, *MATHEMATICA 4.0*, (1999).